Journal of Nuclear Materials 401 (2010) 65–70

Contents lists available at ScienceDirect

Journal of Nuclear Materials

journal homepage: www.elsevier.com/locate/jnucmat

Thermal properties of structural materials used in LWR vessels

J.E. Daw *, J.L. Rempe, D.L. Knudson

Idaho National Laboratory, P.O. Box 1625, MS 4112, Idaho Falls, ID 83415, USA

ARTICLE INFO

Article history:
Received 15 February 2010
Accepted 25 March 2010

ABSTRACT

High temperature thermal property data for structural materials used in existing Light Water Reactors (LWRs) are limited. Often, values extrapolated from available data, as recommended in the literature, differ significantly. To reduce uncertainties in predictions relying upon extrapolated data for LWR vessel and penetration materials, high temperature tests were completed on SA533 Grade B, Class 1 (SA533-B1) low alloy steel, Stainless Steel 304 (SS304), and Inconel 600 using material property measurement systems available in the High Temperature Test Laboratory (HTTL) at the Idaho National Laboratory (INL). Properties measured include thermal expansion, specific heat capacity, and thermal diffusivity for temperatures up to 1200 °C. From these results, thermal conductivity and density were calculated. Results show that, in some cases, previously recommended values for these materials differ significantly from measured values at high temperatures.

1. Introduction

Melt relocation and vessel failure impact the subsequent progression and associated consequences of a Light Water Reactor (LWR) accident. Hence, it is important to accurately predict the heat-up and relocation of materials within the reactor vessel and heat transfer to and from the reactor vessel. However, high temperature thermal property data for structural materials used in Light Water Reactors (LWRs) are limited. A literature review revealed that high temperature properties are often extrapolated because there are little data above 700 °C for these materials. In some cases, extrapolated values (from various sources) were found to differ by more than 20%. To reduce uncertainties in predictions relying upon extrapolated high temperature data, the Idaho National Laboratory (INL) obtained high temperature data for three materials used in LWR vessels: SA533 – Grade B, Class 1 (SA533-B1) low alloy steel, which is used to fabricate most US LWR reactor vessels, and Type 304 Stainless Steel (SS304) and Inconel 600, which are used in LWR vessel piping, penetration tubes, and internal structures. This paper summarizes high temperature thermal property data obtained for these materials.

New high temperature data obtained in this effort and comparisons of the new data with available data in the literature are reported in Section 3. Section 4 summarizes insights from this effort.

2. Methods

Material property data were collected for each material using equipment available at INL's High Temperature Test Laboratory (HTTL). As indicated in Ref. [1], this multi-purpose facility includes equipment such as a pushrod dilatometer, a differential scanning calorimeter, and a laser flash thermal property analyzer required for collecting this data.

Thermal expansion (changes in length caused by changes in temperature) of the test materials was measured using the dilatometer. Assuming that the material is isotropic, the density, ρ, of the material as a function of temperature may be calculated using the equation:

$$\rho = \frac{\rho_0}{1 + 3\frac{\Delta L}{L_0}} \tag{1}$$

where ρ_0 represents the room temperature density, ΔL represents the temperature dependent change in length, and L_0 represents the total sample length at room temperature.

The differential scanning calorimeter (DSC) allows for the measurement of specific heat capacity as a function of temperature. The DSC utilizes a comparative analysis to determine the specific heat of an experimental sample as a ratio of the specific heat of a reference sample.

Thermal diffusivity data were collected using the laser flash thermal property analyzer. Unlike the dilatometer and DSC, the laser flash method does not record data over the entire range of test temperatures. Instead, data are recorded at discrete temperatures (50–100 °C increments are used due to the time required for temperatures to stabilize).

* Corresponding author. Tel.: +1 208 526 7114; fax: +1 208 526 6058.
E-mail address: Joshua.Daw@inl.gov (J.E. Daw).

0022-3115/$ - see front matter © 2010 Published by Elsevier B.V.
doi:10.1016/j.jnucmat.2010.03.022

Thermal conductivity is then found using the relation:

$$k = \rho \cdot \alpha \cdot c_p \quad (2)$$

where k represents thermal conductivity, ρ represents the density, c_p represents the specific heat capacity, and α represents the thermal diffusivity. Note that all quantities are temperature dependent.

3. Results and comparison with existing data

Prior to obtaining new high temperature data, existing data were reviewed, so that new data could be compared with data available in the literature. A review of vessel and structural material properties used to predict phenomena in accident analysis codes reveals that the required high temperature material properties are extrapolated with little, if any, data above 700 °C. Where available, appropriate data are presented for comparison with INL results.

3.1. SA533-B1

Figs. 1–5 compare curve fits based on INL-measured data for SA533-B1 with material property data found in the MATPRO

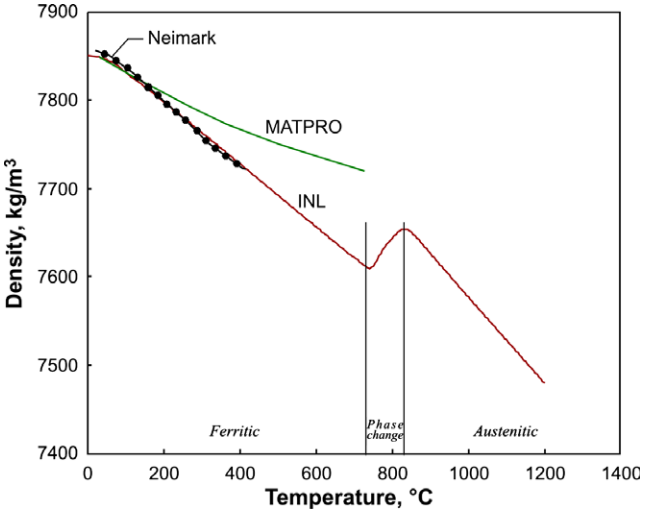

Fig. 1. Temperature dependent density of SA533-B1 carbon steel.

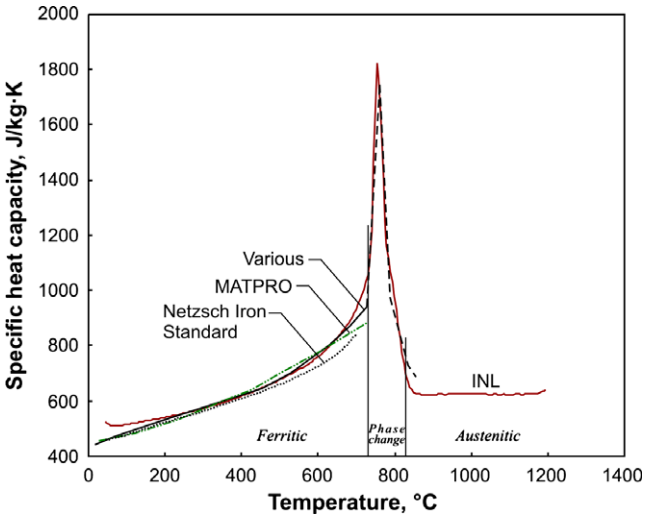

Fig. 3. Temperature dependent specific heat capacity of SA533-B1 carbon steel.

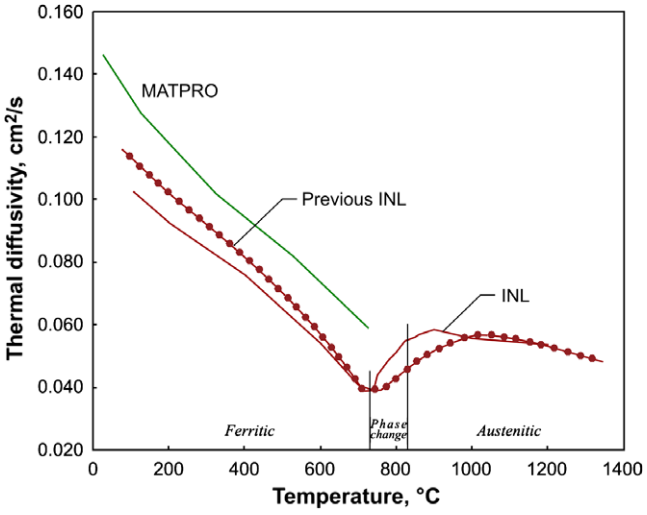

Fig. 4. Temperature dependent thermal diffusivity of SA533-B1 carbon steel.

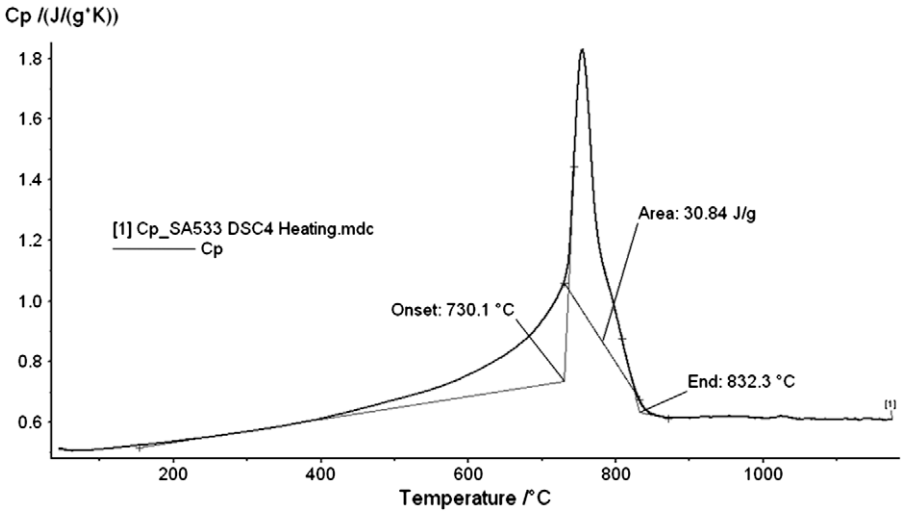

Fig. 2. Phase change approximation for SA533-B1 carbon steel.

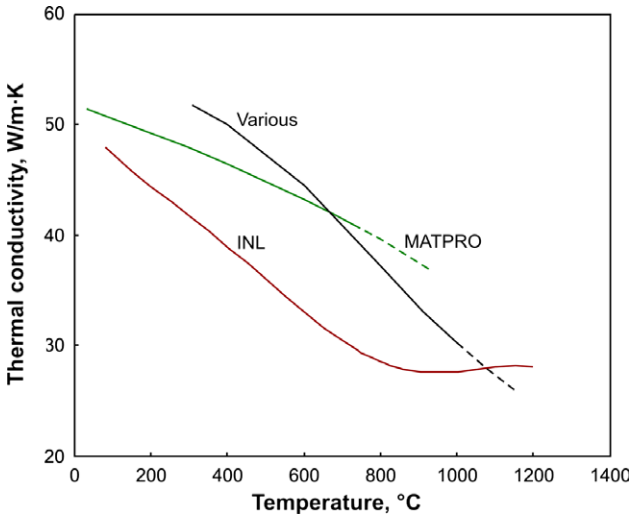

Fig. 5. Temperature dependent thermal conductivity of SA533-B1 carbon steel.

library [2]. MATPRO is the material property data package used in the SCDAP/RELAP5-3D© [3] and MELCOR severe accident analysis codes [4]. MATPRO SA533-B1 data are based on information from Spanner et al. [5]. As appropriate, these figures also include density data from Neimark and Lynsternik [6], specific heat from Netzsch [7] (an iron sample) and Refs. [8–13] (cited as various in figures), and thermal conductivity data [14,15]. Note, all data plotted as dashed lines are extrapolated.

Fig. 1 shows a density curve obtained by INL for SA533-B1 low alloy carbon steel, This curve was derived from the measured thermal expansion using Eq. (1). INL results are lower by up to 1.4% (106.3 kg/m^3) than the MATPRO curve, which was based on data obtained for temperatures below 730 °C. INL data are in close agreement with Neimark data, which are limited to temperatures below 427 °C.

Fig. 2 shows a curve obtained from average specific heat capacity data for SA533-B1 low alloy carbon steel collected at the HTTL. Estimated latent heat and bounding temperature values are also shown in plot. The large spike in the INL results corresponds to the solid state phase change (also observed in the thermal expansion data) experienced by this material when it transitions from ferritic to austenitic steel. The curve indicates how energy is absorbed by the sample as it is heated (specific heat capacity is the amount of energy required to cause a temperature change). During the phase change, much of this energy is used in restructuring of the material. This spike, therefore, is not a good indicator of the true specific heat of the sample in the temperature range of the phase change. To account for this, the DSC manufacturer recommends interpolating between the onset and end temperatures of the phase change, using either a linear or tangential interpolation, to calculate the specific heat. This is accomplished using software provided with the DSC. The temperature limits are not easy to define from the DSC data, however. The onset of a phase change during a heating cycle is useful, but the end temperature may be difficult to estimate. To estimate the temperature range that corresponds to the phase change, values were determined using thermal expansion data from dilatometer measurements. Using a linear interpolation, the specific heat during phase change was estimated, as was the latent heat of phase change (the area under the spike).

Fig. 3 compares the INL-obtained specific heat data curve with results in the literature. Results collected at temperatures below the phase change onset differ from MATPRO values by a maximum of 16.1% (170.6 J/kg K) and differ from data given in Refs. [8–13] by 10.8% (114.4 J/kg K).

Fig. 4 shows data collected for SA533-B1 thermal diffusivity. Also shown are results published in the MATPRO library and data from previous INL [16] tests. Again, there is a significant change in behavior apparent in the temperature range in which phase change occurs. Data from INL tests are in close agreement, though there is an offset from the MATPRO data, with a maximum difference of 31.7% (0.019 cm^2/s).

Thermal conductivity results for SA533-B1 are compared with results published in other references in Fig. 5. INL data were calculated using Eq. (2). As discussed above, INL values for thermal conductivity in the temperature range associated with phase change should be considered approximate. There is a clear change in behavior between the ferritic and austenitic phases, as the slope of the thermal conductivity curve changes. The maximum difference between INL and MATPRO data occurs just below the onset of phase change (MATPRO data are extrapolated above this temperature). This difference is 11.9% (4.4 W/m K).

3.2. SS304

Figs. 6–9 show stainless steel 304 material property results published by Touloukian et al. [17] (extrapolated for values over

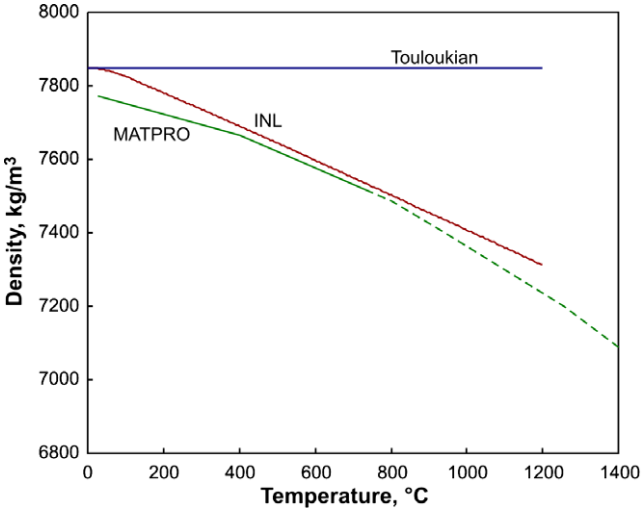

Fig. 6. Temperature dependent density of SS304 stainless steel.

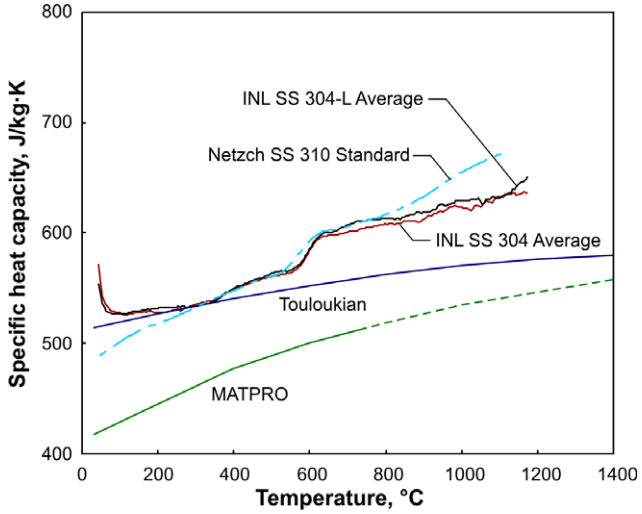

Fig. 7. Temperature dependent specific heat capacity of SS304 stainless steel.

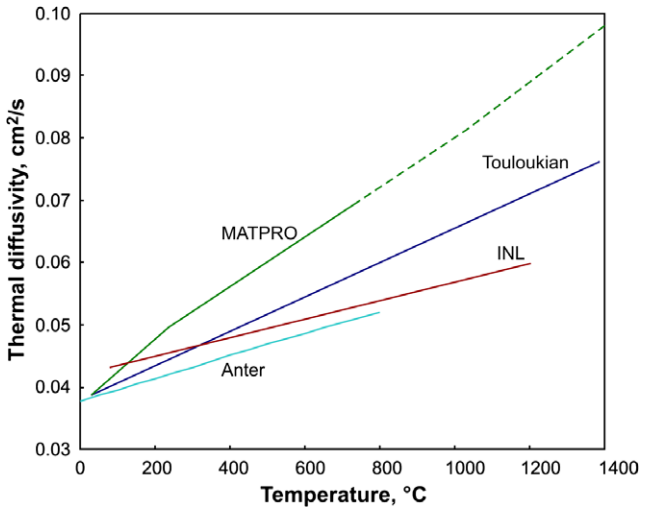

Fig. 8. Temperature dependent thermal diffusivity of SS304 stainless steel.

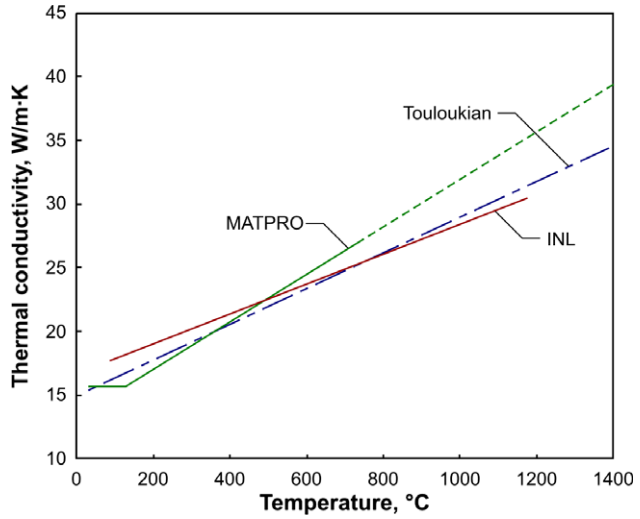

Fig. 9. Temperature dependent thermal conductivity of SS304 stainless steel.

1000 °C), as well as curves published in the MATPRO library (MATPRO stainless steel density, thermal conductivity, and specific heat curves are extrapolated for temperatures above 1000 °C; thermal diffusivity data are based on data collected by Peckner and Berstein [18], and are extrapolated for temperatures above 730 °C). Also presented are specific heat capacity results from Netzsch [7] and thermal diffusivity results from Anter [19].

Fig. 6 shows density results for 304 stainless steel derived from the measured thermal expansion data using Eq. (1). The maximum difference between MATPRO and INL results is 1.02% (74.3 kg/m^3), while the maximum difference between INL and Touloukian values is 7.3% (535.3 kg/m^3).

Fig. 7 shows average specific heat capacity results for 304 and 304 L stainless steel collected at the HTTL (measured using a differential scanning calorimeter). INL results closely match the Netzsch standard results. Furthermore, INL results are very close to results published in Touloukian for temperatures up to approximately 600 °C, at which point the INL and Netzsch results show a slight "bump." This bump at 600 °C is indicative of carbide formation. The maximum difference between INL and Touloukian results is 10.4% (59.8 J/kg K) at 1200 °C, the maximum temperature for which INL data were obtained. The difference between INL and MATPRO data, approximately constant over the temperature range of INL data, is 18% (85 J/kg K).

Fig. 8 shows INL results for 304 stainless steel thermal diffusivity. Also shown are results from Touloukian, Anter, and the MATPRO library. INL results (both from recent and earlier tests) are consistent with the Anter and Touloukian values (Touloukian values were extrapolated above 1000 °C) differing from Anter results by a maximum of 2.7% (0.0015 cm^2/s) and from Touloukian results by 16.9% (0.012 cm^2/s). The INL results also match the MATPRO values for lower temperatures but are much lower at high temperatures (MATPRO values were extrapolated above 730 °C), with a maximum difference of 33.6% (0.03 cm^2/s).

Fig. 9 shows the calculated (from Eq. (1)) thermal conductivity of 304 stainless steel. Also shown are results from Touloukian and MATPRO. Despite some differences in the measured property values for thermal expansion, thermal diffusivity, and specific heat capacity used to calculate thermal conductivity, INL results are in close agreement with both literature sources (both of which were extrapolated for temperatures above 1000 °C). At 1000 °C, INL results differ from MATPRO values by 13.43% (4.3 W/m K) and from Touloukian values by 4.7% (1.4 W/m K). At 1200 °C INL values differ from MATPRO values by 13.40% (4.8 W/m K) and from Touloukian values by 2.9% (0.9 W/m K).

3.3. Inconel 600

Figs. 10–13 show Inconel 600 material property results published by Touloukian [20] as well as manufacturers Special Metals, Incorporated (density described as a physical constant) [21] and Huntington Alloy [22]. Also shown are specific heat capacity values from Netzsch [7], and density results from Air Force studies [23]. Curves based on extrapolated data are plotted with a dashed line.

Fig. 10 shows INL density results for Inconel 600. Results from Touloukian were calculated from thermal expansion data in the same manner as INL data, as thermal expansion data were available but density data were not. INL results closely match Touloukian results differing by a maximum of 0.5% (43.5 kg/m^3). INL results also match the trend shown in Air Force results; though the Air Force values are consistently lower by approximately 3.9% (330 kg/m^3).

Fig. 11 shows specific heat capacity results for Inconel 600 collected at the HTTL (measured using a differential scanning calorimeter). The results obtained by INL closely match values found in the literature. INL results differ from Netzsch results by a maximum of

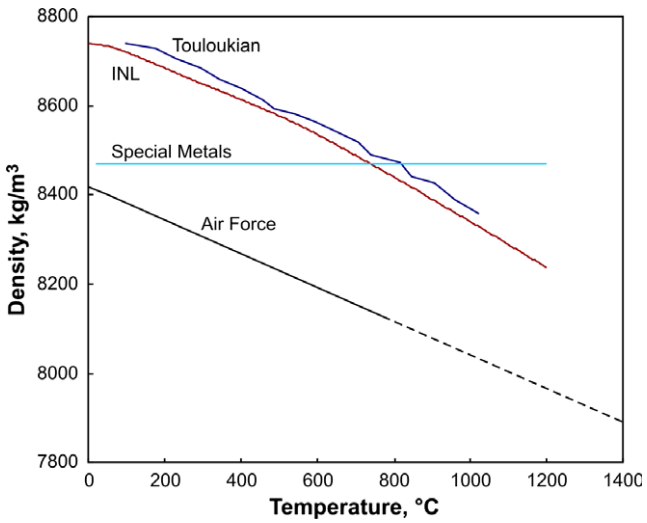

Fig. 10. Temperature dependent density of Inconel 600.

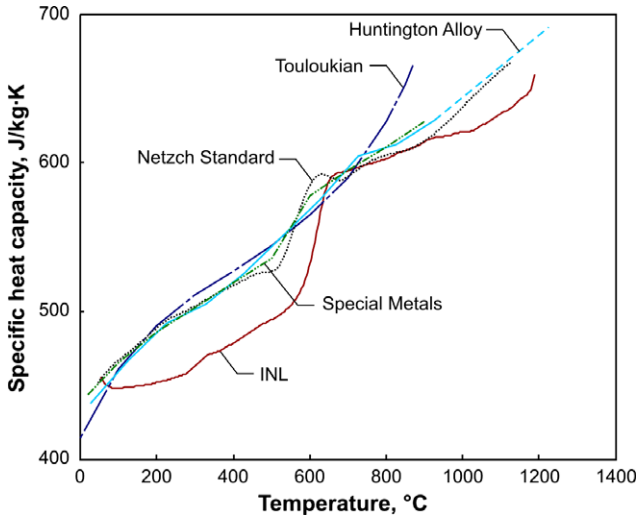

Fig. 11. Temperature dependent specific heat capacity of Inconel 600.

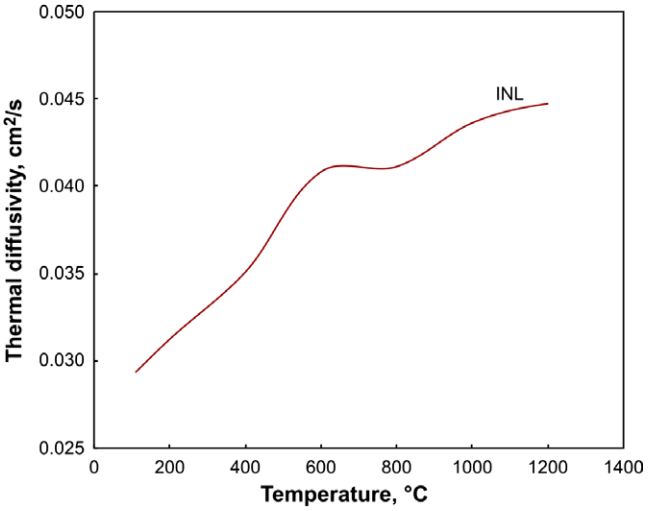

Fig. 12. Temperature dependent thermal diffusivity of Inconel 600.

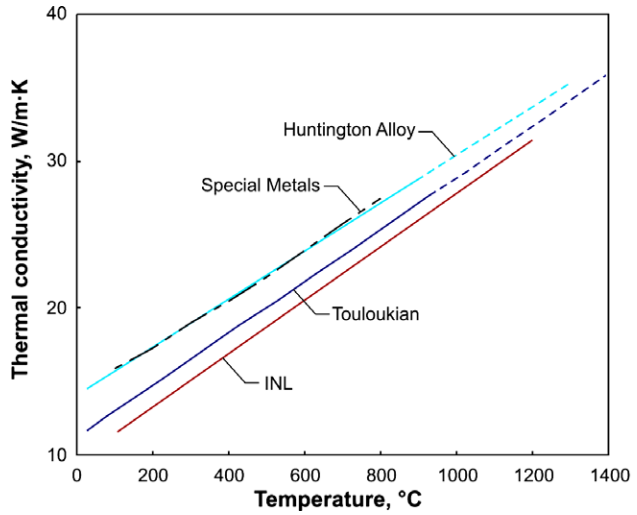

Fig. 13. Temperature dependent thermal conductivity of Inconel 600.

10.2% (58.7 J/kg K) and from Touloukian results by a maximum of 8.3% (55.1 J/kg K). Results from INL Netzsch and Special Metals show a "bump" in specific heat between 500 and 700 °C corresponding to formation of $NiCr_3$ clusters [24].

Fig. 12 shows INL thermal diffusivity results for Inconel 600. No reference values were found for comparison. The INL results exhibit a "bump" in the same temperature range as that seen for specific heat; this may also be associated with $NiCr_3$ cluster formation.

Fig. 13 compares thermal conductivity results calculated for Inconel 600 with results obtained from Touloukian and manufacturers Special Metals and Huntington alloy. INL data are consistent with reference sources, differing from Touloukian results by an average of 1.4% (8.5 W/m K).

4. Summary

Thermal property data for SA533-B1 low carbon steel, 304 stainless steel, and Inconel 600 were collected at Idaho National Laboratory's High Temperature Test Laboratory. Data for thermal expansion, specific heat capacity, and thermal diffusivity up to 1200 °C were obtained. These data were used to calculate density and thermal conductivity, which were then compared to results found in the literature. SA533-B1 exhibited a solid state phase change between temperatures of approximately 740 and 840 °C. Although this behavior significantly affected INL results, few examples in the literature indicate the presence of this behavior. It is also interesting to note that although much of the thermal expansion, thermal diffusivity, and specific heat capacity data collected for 304 stainless steel and Inconel 600 differed from literature sources, the resulting thermal conductivity values were very close to accepted values.

Product disclaimer

References herein to any specific commercial product, process, or service by trade name, trademark, manufacturer, or otherwise, does not necessarily constitute or imply its endorsement, recommendation, or favoring by the U.S. Government, any agency thereof, or any company affiliated with the Idaho National Laboratory.

Acknowledgment

This work was supported by the U.S. Department of Energy, Office of Nuclear Energy, Science, and Technology, under DOE-NE Idaho Operations Office Contract DE AC07 05ID14517.

References

[1] High Temperature Test Laboratory. Available from: <www.inl.gov/httl/>, Last visited January 15, 2010.
[2] Idaho National Engineering and Environmental Laboratory, SCDAP/RELAP5-3D© Code Manuals, vol. 4, MATPRO-A Library of Materials Properties for Light-Water-Reactor Accident Analysis, INEEL/EXT-02-00589, Idaho National Engineering and Environmental Laboratory, May 2002.
[3] Idaho National Engineering and Environmental Laboratory, SCDAP/RELAP5-3D© Code Manuals, vols. 1–4, INEEL/EXT-02-00589, Idaho National Engineering and Environmental Laboratory, May 2002.
[4] Sandia National Laboratories, MELCOR Computer Code Manuals, NUREG/CR-6119, vols. 1–3, SAND2001-0929P, May 2001.
[5] J.C. Spanner et al., Nuclear Systems Material Handbook, TID-26666, April 1976.
[6] B.E. Neimark, V.E. Lynsternik, Teploenergetika 7 (1960) 16–18.
[7] NETZSCH Proteus Thermal Analysis, Version 4.8.5, Selb, Germany, NETZSCH, 2008.
[8] J.H. Awbery, A.R. Challoner, P.R. Pallister, R.W. Powell, Journal of the Iron Steel Institute 154 (2) (1946) 83–111.
[9] P.R. Pallister, Journal of the Iron Steel Institute 185 (4) (1957) 474–482.
[10] British Iron and Steel Research Association, Physical Constants of Some Commercial Steels at Elevated Temperatures, Butterworth's Scientific Publication, Ltd., London, 1953, p. 38.
[11] E. Griffiths, R.W. Powell, M.J. Hickman, The Physical Properties of a Series of Steels – I, Special Report No. 24, Iron Steel Institute, London, 1939.

[12] E.G. Shuidkovskii, Journal of Technical Physics 8 (1938) 935–947.
[13] G.V. Smith, Evaluations of the Elevated Temperature Tensile and Creep Rupture Properties of C–Mo, Mn–Mo, and Mn–Mo–Ni Steels, Metal Properties Council, American Society for Testing and Materials, ASTM Data Series Publication DS47, 1971.
[14] K. Honda, T. Simidu, Science Reports of Tohoku University 6 (1917–1918) 219–234.
[15] D.L. Timrot, Zhurnal Tekhinicheskoi Fisiki 5 (1935) 1011–1036.
[16] J.L. Rempe, D.L. Knudson, Journal of Nuclear Materials 372 (2008) 350–357.
[17] Y.S. Touloukian et al., Thermophysical Properties of Matter, IFI/Plenum Publishing, New York, NY, 1973.
[18] D. Peckner, I.M. Berstein (Eds.), Handbook of Stainless Steel, McGraw-Hill Book Company, New York, 1977, pp. 19-3–19-26.
[19] Anter Laboratories, Inc., Declarations of Reference Material Conformity, Pittsburgh, PA.
[20] Y.S. Touloukian, Thermophysical Properties of Matter, IFI/Plenum Publishing, New York, NY, 1970.
[21] Special Metals Inc., Inconel Alloy 600. Available from: <http://www.specialmetals.com/products/inconelalloy600.php/>, Publication No. SMC-027, published September 20, 2008, Web page visited February 18, 2009.
[22] Huntington Alloy, Inconel Alloy 600, Technical Bulletin of the International Nickel Company, Inc., Huntington Alloy Products Division, seventh ed., Huntington, WV, 1978.
[23] Aerospace Structural Metals Handbook, Air Force Materials Laboratory, 1990 ed., Revised December 1990.
[24] NETZSCH., Nickel Based Super Alloy (Inconel Alloy 600), 103-2006-LFA457-Metals-Aerospace-Inconel600[1].pdf, Publication No. AS-103-2006, Web page visited July 2, 2009.